Supplement of Atmos. Chem. Phys., 18, 16809–16828, 2018
https://doi.org/10.5194/acp-18-16809-2018-supplement

Atmospheric Chemistry and Physics
Open Access
EGU

Supplement of

Cloud impacts on photochemistry: building a climatology of photolysis rates from the Atmospheric Tomography mission

Samuel R. Hall et al.

Correspondence to: Michael J. Prather (mprather@uci.edu)

Contents of this file

This Supplementary Material includes figures and tables referenced in the main text and useful for understanding this work, but not essential to its findings.

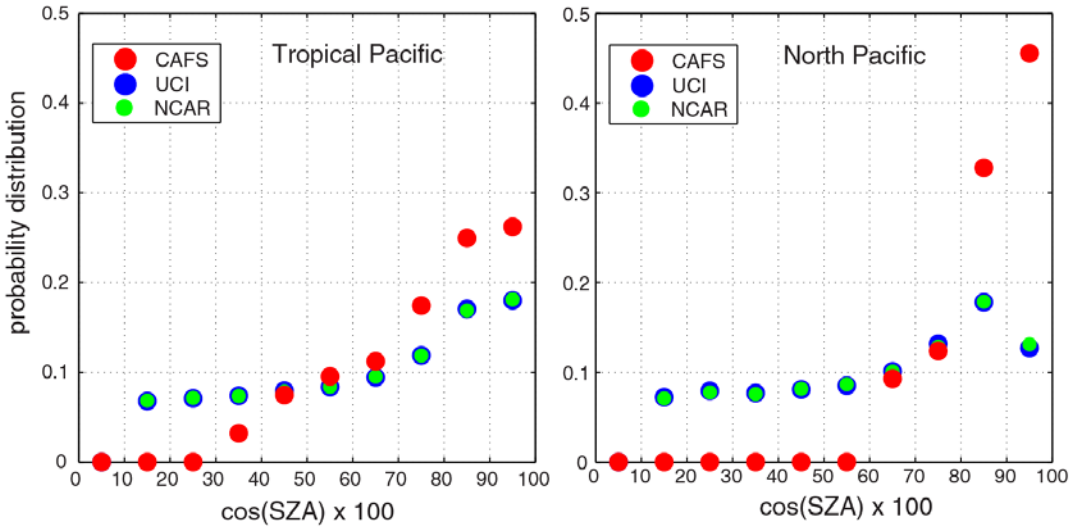

Figure S1. The probability distribution of solar zenith angles (SZAs) as sampled by ATom with the CAFS instrument (red) and by two models (UCI & NCAR) using regular sampling over the two geographic blocks: (1, left) Tropical Pacific and (2, right) North Pacific. The points represent the relative number of samples in each 0.10 interval of cos(SZA). ATom flights in this region were generally centered about noon, and hence CAFs has a higher proportion of high cos(SZA) values. For most of the analysis here only J's with cos(sza) > 0.8 are used, and with this restriction the number of CAFS measurements is 11,504 (block 1) and 4,867 (block 2). For UCI the number of points is 240,000 (block 1) and 120,000 (block 2); while for the higher resolution NCAR model, the values are 1,400,000 and 700,000, respectively.

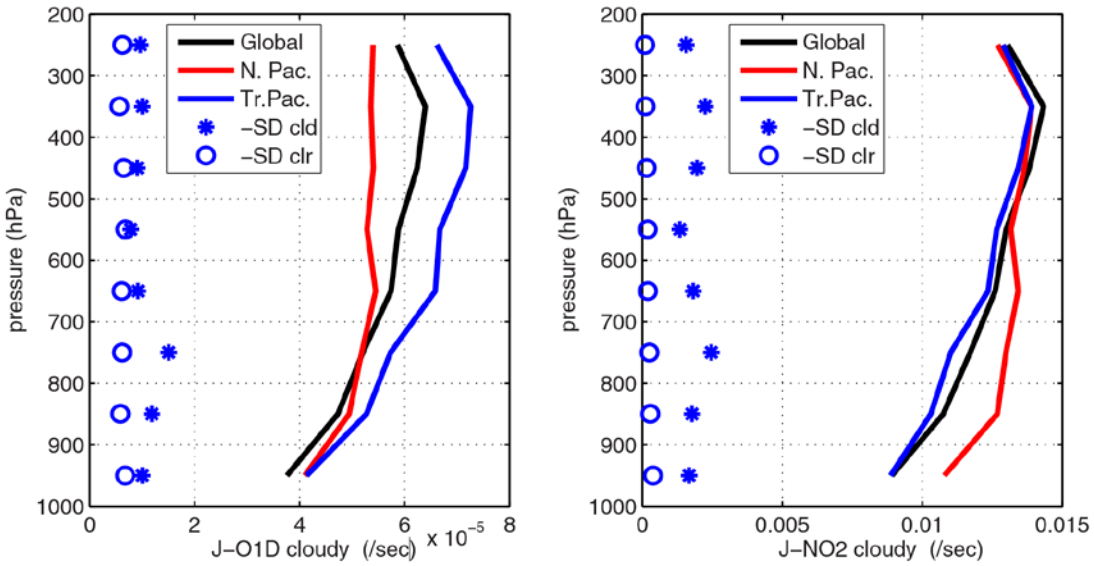

Figure S2. Mean CAFs profiles of J-O1D (left) and J-NO2 (right) from ATom-1 made under all-sky conditions for high-sun conditions, cos(sza) > 0.8. The 3 geographic blocks shown here are the standard blocks 1 (blue, Tropical Pacific, 20 ºS – 20 ºN x 160 ºE – 240 ºE), and 2 (red, North Pacific, 20 ºN – 50 ºN x 170 ºE – 225 ºE, plus a global block (black, 55 ºS – 55 ºN, all longitudes, including the Atlantic). Each 3-sec observation is averaged with equal weight in 100-hPa pressure bins. The standard deviation for block 1 (blue, *) is shown along with that from the corresponding TUV model calculation for clear sky (blue, o). The patterns here are expected: J-O1D is sensitive to O_3 absorption and hence has higher upper-tropospheric values in the tropics; J-NO2 is more sensitive to cloud scattering and hence has higher values in the lower troposphere of the North Pacific. The standard deviations show that J-O1D variance is driven by O_3 and SZA, and not by clouds; while the J-NO2 shows the opposite.

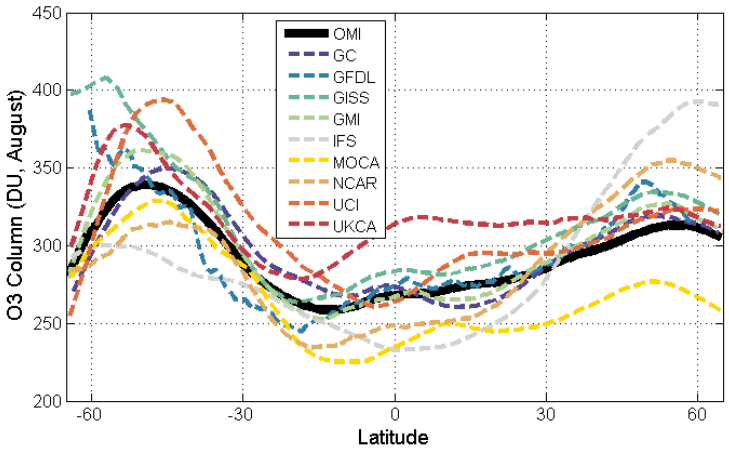

Figure S3. Total ozone columns (in DU) versus latitude in August for 9 models and 8 years of OMI observations (2010-2017, Levelt et al., 2006; Veefkind et al., 2006). Most curves are the monthly zonal means, but some data are from a single day, or just the ATom flight track for several days (e.g., GFDL, explains the lack of smoothness). Differences here can explain only some of the spread in clear-sky J-O1D values in Figure 2.

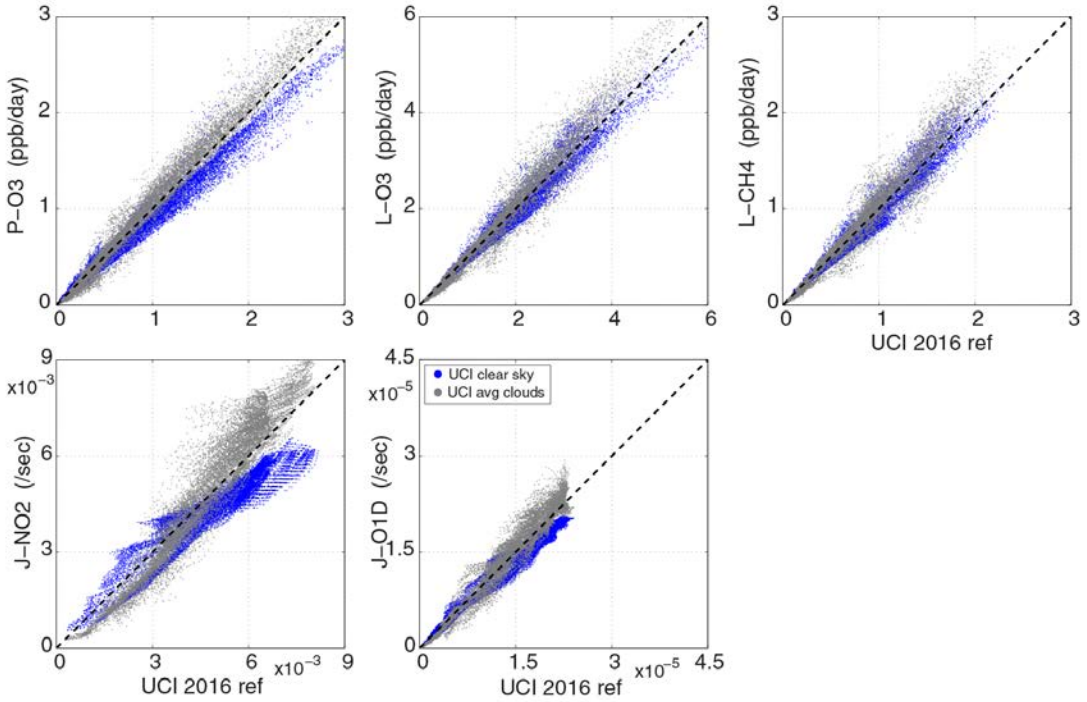

Figure S4. Effects of clear sky (blue points), simple averaged clouds (gray points), and fractional cloud overlap (the reference case, 1:1 dashed line) using the UCI CTM. X-axis is the same as the Y-axis, but for the reference model UCI 2016. Direct parcel-by-parcel comparison of modeled 24-hour reactivities (top row: P-O3, L-O3, L-CH4; all ppb/day) and photolysis rates (J-NO2, J-O1D; all /sec) calculated for a data stream of 14,880 simulated air parcels from 60 ºS to 60 ºN, 0.5 km to 12 km altitude, and along 180 ºW, see Prather et al., 2018. Each point is an average of the 5 simulated dates in August (8/01, 8/06, 8/11, 8/16, 8/21). UCI 2016 ref uses full cloud quadrature and the newly implemented decorrelation lengths for cloud overlap (Prather, 2015). From the figure, the different cloud treatments are clearly visible in the shifts in J-NO2 and J-O1D, and they have largest effect on P-O3 as compared with L-O3 and L-CH4. On average, the clear-sky simulation has 3-4% lesser J-values and similar changes in all 3 reactivities. The averaged-cloud method has about 12 % greater J-values (mostly above clouds), increasing reactivities by 5 % (L-O3 and L-CH4) to 10% (P-O3).

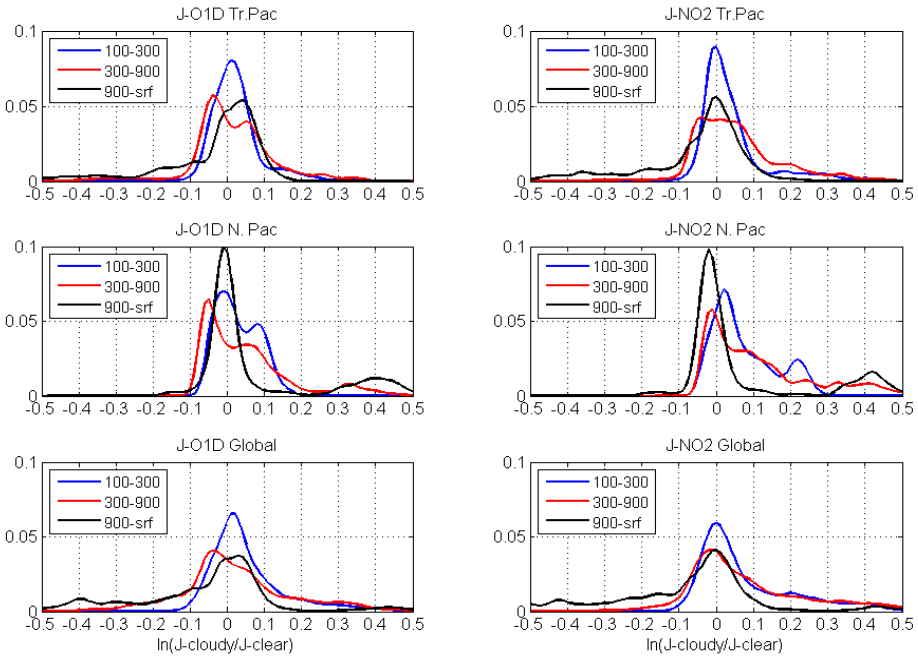

Figure S5. Histogram of the natural log of the ratio of cloudy-to-clear J values (J-O1D & J-NO2), designated rlnJ, which is calculated from the 10-sec CAFS data and sorted into 3 pressure bins (blue, 100 – 300; red, 300 – 900; black, 900 – surface hPa). Note that the upper level has a peak near 0.0, corresponding to clear sky; the lowest level extends more to values <0; and that the N. Pacific for <900 hPa has a large number of cloud enhanced J-values (rlnJ >0). The CAFS data were binned at 0.01 rlnJ and smoothed with a 1-2-1 filter six times.

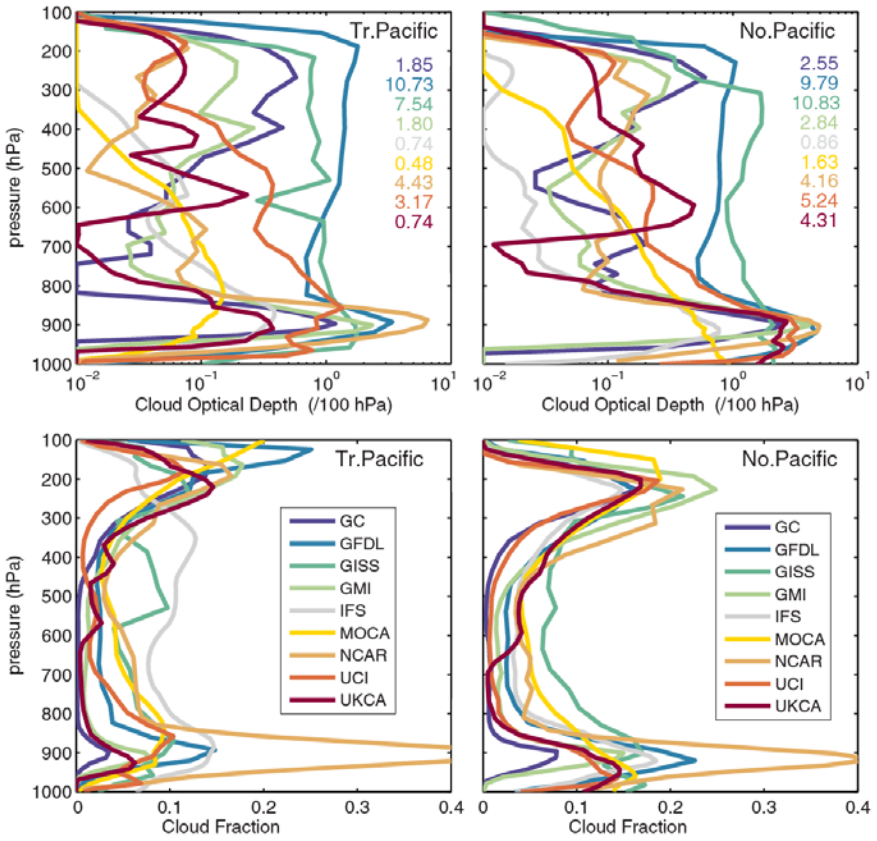

Figure S6. Averaged in-cell cloud optical depth (COD, at ~600 nm and per 100 hPa) and cloud fraction (CF) over the two geographic blocks studied here (Tropical Pacific, 20 ºS – 20 ºN x 160 ºE – 240 ºE, and North Pacific, 20 ºN – 50 ºN x 170 ºE – 225 ºE). Averages are made over 24 hours for one day in mid-August as used in this paper. For these data (unlike the J-value statistics), all hours are weighted equally independent of solar zenith angle. Column total COD for each region is given in the order/color-indexed numbers on the right of each COD panel.

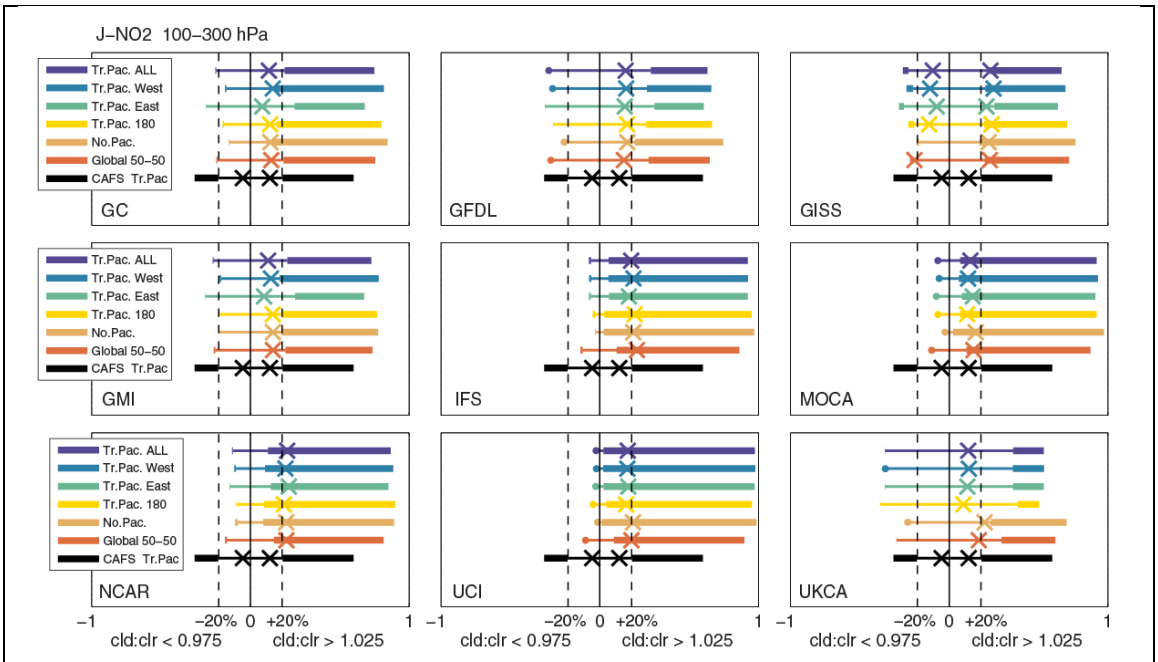

Figure S7a. The effect of sampling different regions of the tropical Pacific in terms of the frequency of occurrence and magnitude of changes caused by clouds in J-NO2 at 100-300 hPa. See Figure 5. Each of the 9 panels shows a single model with different sampling and also the CAFS observations over the tropical Pacific (bottom black bar and X's). The top purple bar is the entire tropical Pacific as defined in Figure 5 (20S-20N, 160E-240E) and the next three bars (blue, green, yellow) sub-sample this region into West (160E-200E), East (200E-240E) and 180E (175E-185E), respectively. The next two bars are the North Pacific (as in Figure 5) and a global sampling (50S-50N, all longitudes).

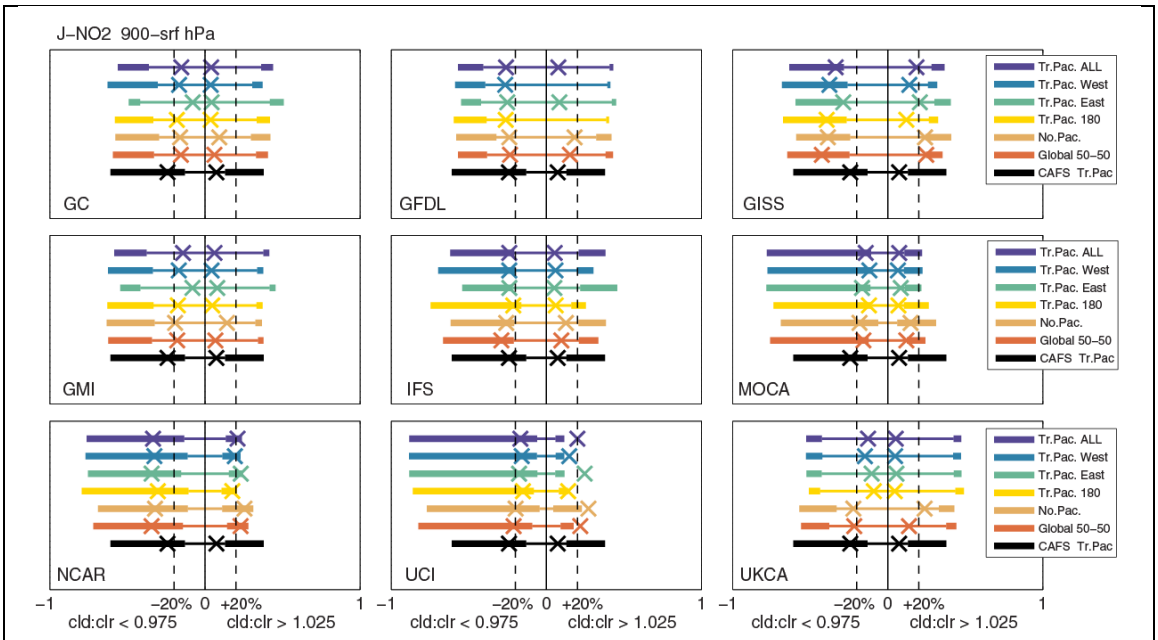

Figure S7b. The effect of sampling different regions of the tropical Pacific in terms of the frequency of occurrence and magnitude of changes caused by clouds in J-NO2 at surface-900 hPa. See Figure S7a.

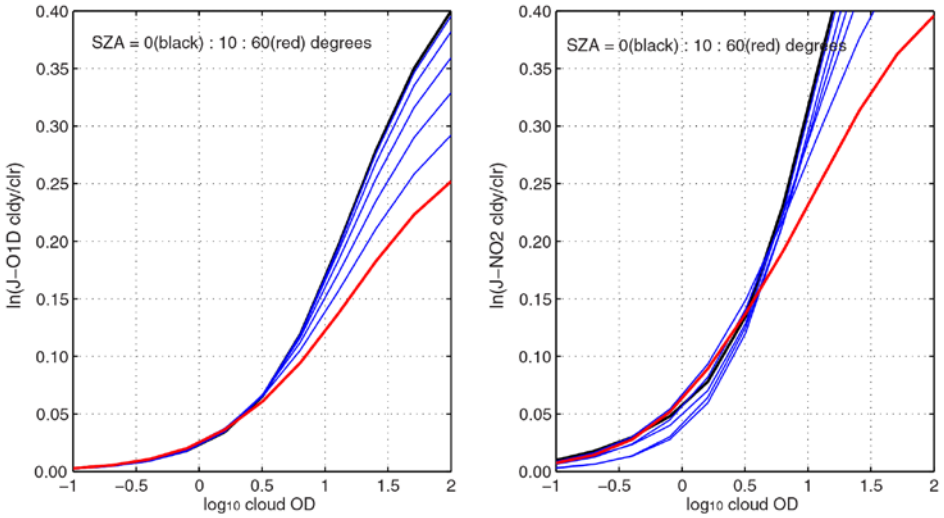

Figure S8. The ratio of J-cloudy/J-clear calculated for J-O1D (left) and J-NO2 (right) at 300 hPa for a marine stratus cloud (CF = 100%) at about 900 hPa. The natural log of the ratio (rlnJ) is calculated for a cloud optical depth (COD) ranging from 0.1 to 100. The calculation uses Cloud-J (Prather, 2015), which does not scale COD, uses the truncated (order 8) phase function, and applies a constant lower boundary albedo = 0.05. The incident SZA ranges from 0º (black) to 60º (red) in 10º intervals (blue). The rlnJ's in this paper are restricted to 0º – 40º. A 5 % enhancement (rlnJ = 0.05) occurs at COD = 2 for J-O1D and COD = 1 for J-NO2, demonstrating the greater sensitivity of J-NO2 to clouds.

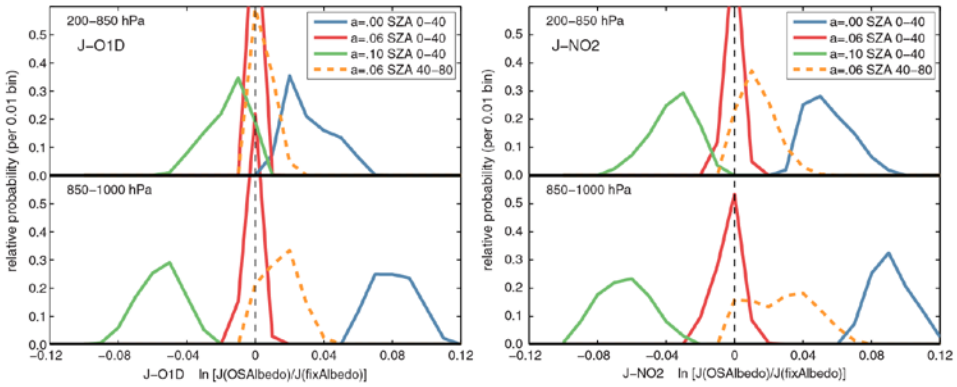

Figure S9. Probability distribution of the natural log of the ratio of J-values calculated using an interactive ocean surface albedo (OSA) to J-values using a fixed albedo. J-O1D values (left) and J-NO2 values (right) assume clear skies for both OSA and fixed-albedo. This format is similar to Figure 4. The interactive OSA model includes a dependence on wavelength and incident-angle now in Cloud-J v8, see text. The fixed albedo is denoted by 'a =' in the legend. These distributions show the relative error in J-values calculated in typical models using a fixed albedo instead of the more physically based OSA models (Séférian et al., 2018). For both cases the reflected sunlight is assumed to be isotropic. The OSA depends on surface wind (sampled uniformly from 1 to 21 m/s) and chlorophyll abundance (sampled uniformly in log from 0.01 to 30 mg/m^3). The plots are also split between the lowermost troposphere (lower panels, >850 hPa) and free troposphere (upper, 200 – 850 hPa).

Table S1. Model contact information			
short name	long name	POCs for these simulations	
CAFS	---	Sam Hall <halls@ucar.edu>	Kirk Ullmann <ullmannk@ucar.edu>
GC	GEOSChem	Murray, Lee <lee.murray@rochester.edu>	
GFDL	GFDL AM3	Arlene Fiore <amfiore@ldeo.columbia.edu>	Gustavo Correa <gus@ldeo.columbia.edu>
GISS	GISS ModelE2	Murray, Lee <lee.murray@rochester.edu>	
GMI	GSFC GMI	Sarah A. Strode <Sarah.A.Strode@nasa.gov>	Stephen Steenrod <Stephen.D.Steenrod@nasa.gov>
IFS	ECMWF IFS	Johannes Flemming <johannes.flemming@ecmwf.int>	Vincent Huijnen <vincent.huijnen@knmi.nl>
MOCA	MOCAGE	Beatrice Josse <beatrice.josse@meteo.fr>	Jonathan Guth <jonathan.guth@meteo.fr>
NCAR	CESM	Jean-Francois Lamarque <lamar@ucar.edu>	
UCI	UCI CTM	Michael Prather <mprather@uci.edu>	Clare Flynn <claref@uci.edu>
UKCA	UKCA	Luke Aabraham <luke.abraham@atm.ch.cam.ac.uk>	Alex Archibald <ata27@cam.ac.uk>, Marcus Koehler <m.koehler@uea.ac.uk>